

# Monitoring the dynamics of an open quantum system via a single qubit

P. C. López Vázquez<sup>1</sup> and T. Gorin<sup>2</sup>

<sup>1</sup>*Departamento de Ciencias Naturales y Exactas, Universidad de Guadalajara, Carretera Guadalajara - Ameca Km. 45.5 C.P. 46600. Ameca, Jalisco, México.*

<sup>2</sup>*Departamento de Física, Universidad de Guadalajara, Blvd. Marcelino García Barragán y Calzada Olímpica, C.P. 44840, Guadalajara, Jalisco, México.*

We investigate the possibility to monitor the dynamics of an open quantum system with the help of a small probe system, coupled via dephasing coupling to the open system of interest. As an example, we consider a dissipative harmonic oscillator and a single qubit as probe system. Qubit plus oscillator are described by a finite temperature quantum master equation, where the dynamics of the whole system can be obtained analytically. We find that the short time behavior of the reduced qubit state (its coherence) provides exhaustive information on the dissipative dynamics of the oscillator. Observing this coherence for two initial states with different out-of-equilibrium temperatures, one can determine all coupling constants and the equilibrium temperature fixed by the external heat bath. In addition, the dephasing coupling to the qubit probe, may be considered as a perturbation of the dissipative oscillator. The corresponding quantum fidelity can be calculated analytically, also. Hence, we find the precise relation between the behavior of the reduced qubit state (its coherence) and that fidelity.

## I. INTRODUCTION

The idea of probing the dynamics of a quantum system by another smaller quantum system coupled to the first one, goes probably back to Gardiner, Cirac and Zoller [1]. In that paper, the authors propose to study the stability of the unitary dynamics of a complex, eventually quantum chaotic system, the delta-kicked harmonic oscillator, using a probe degree of freedom coupled to the system by dephasing. That stability is characterized in terms of the quantum fidelity (“quantum Loschmidt echo”) [2–5].

More recently, quantum thermodynamics has drawn a lot of attention in part due to the difficulties which occur when one tries to extend the classical thermodynamic concepts such as work, heat, entropy, and thermalization to small microscopic quantum systems [6–9]. There, it is of fundamental interest to develop accurate techniques for the verification of thermodynamical properties. In this sense, “quantum thermometry” has been formulated for single qubit readouts [10, 11]. Further work in this direction has been centered on the construction of quantum heat machines [12–16].

The purpose of the present work consists in extending the original scheme for probing quantum fidelity to the case of dissipative dynamics. Thereby, we want to understand how to extract as much information as possible about the dissipative dynamics in question. For the quantum chaotic case, some results have been obtained in Ref. [17] in the case of an infinite temperature bath. Here, we are interested in the case of finite temperature and a finite coupling strength (dissipation rate), and instead of a quantum chaotic system as in Ref. [18], we study a simple harmonic oscillator. This allows us to obtain the dynamics of the full system analytically, and thereby study the relations between the dynamics of the oscillator and that of the quantum probe in every detail.

Dephasing coupling has been studied in many different contexts [19–23]. The qubit-oscillator system with de-

phasing coupling could be implemented experimentally, with superconducting quantum devices [24–26], trapped ions [27–30], ultracold atoms in an optical lattice [31–34], Josephson junctions [35, 36], or defect centers in solid-state crystals [37].

The dissipative harmonic oscillator has the extraordinary feature that Gaussian wave packets continue to evolve as Gaussian wave packets for all times. Following Refs. [38, 39] this allows us to compute Uhlmann’s [40] (Jozsa’s [41]) fidelity for mixed quantum states in analytical form. We then compare the generalized fidelity which has been introduced in Ref. [17] and is based on the qubit coherence, with the standard fidelity for mixed quantum states. In Refs. [42–44] discuss different possibilities to extract information about the dynamics of an oscillator with the help of coupled to the system.

The paper is organized as follows: In Sec. II the details about our tripartite model, together with the definitions of the generalized fidelity and the Uhlmann-Jozsa fidelity are given. Also we give a short review about the Wigner function description and state some of the properties of its two dimensional Fourier transform or the chord function. In Sec. III, we derive an analytic solution for the dynamics of our model system, and discuss the reduced dynamics of the oscillator and the qubit. In Sec. IV, we find analytical expressions for the generalized fidelity and the Uhlmann-Jozsa fidelity, as well as the connection formulas between the two fidelities and the purities of the qubit and the oscillator; furthermore, we use our previous results to propose a method to implement a quantum thermometer by looking only at the decoherence decaying rate of the qubit. Finally in Sec. V we give our conclusions.

## II. THE TRIPARTITE SYSTEM

The system is composed of three parts; a central two-level system (qubit), an intermediate harmonic oscillator and a heat bath of finite temperature, whose effect is described by a quantum master equation of Lindblad form. Assuming a quantum optical setting, and measuring energy in units of  $\hbar\omega_o$ , the energy quantum of the oscillator, and time in units of  $\omega_o^{-1}$ , we may write the master equation in terms of dimensionless quantities

$$i \frac{d\rho}{dt} = [H, \rho] + i\mathcal{L}[\rho], \quad (1)$$

where the density matrix  $\rho$  represents the mixed state of qubit plus oscillator mode. The Hamiltonian is divided into the qubit part, the oscillator part  $H_{\text{osc}}$ , and the coupling between both systems:

$$H = \frac{\Delta}{2} \sigma_z + H_{\text{osc}} + g \sigma_z \otimes \hat{x}, \quad (2)$$

$$H_{\text{osc}} = \frac{1}{2} (\hat{x}^2 + \hat{p}^2) = \hat{a}^\dagger \hat{a} + \frac{1}{2}. \quad (3)$$

The mixed state of the qubit alone is obtained from  $\rho$  via the partial trace. In our model, the coupling is of the dephasing type. Therefore, the populations of the qubit states are constant in time, and the non-diagonal element of the qubit density matrix (“coherence”) is the quantity of interest, as it contains all the information about the dynamics of the oscillator. The Lindblad term, which accounts for the dissipative processes, is given by

$$\mathcal{L}[\rho] = -\kappa (1 + \bar{n}) (a^\dagger a \rho - 2 a \rho a^\dagger + \rho a^\dagger a) - \kappa \bar{n} (a a^\dagger \rho - 2 a^\dagger \rho a + \rho a a^\dagger), \quad (4)$$

where  $\kappa = \gamma_o/\omega_o$ . Here,

$$\bar{n} = \langle \hat{a}^\dagger \hat{a} \rangle_{\rho_T} = \frac{1}{e^{1/D} - 1}, \quad (5)$$

is the average number of excitations, and  $\rho_T$  the canonical equilibrium state of the harmonic oscillator at temperature  $T$ . The parameter  $D = k_B T / (\hbar \omega_o)$  is the dimensionless diffusion constant from the quantum Brownian motion model [45].

### A. Fidelities

The density operator  $\rho$ , which appears in Eq. (1), describes the mixed quantum state of the bipartite system consisting of two-level system (qubit) and harmonic oscillator. It may be written in block-matrix form as follows:

$$\rho(t) = \begin{pmatrix} a_{00} \rho_{00}(t) & a_{01} \rho_{01}(t) \\ a_{10} \rho_{10}(t) & a_{11} \rho_{11}(t) \end{pmatrix}, \quad (6)$$

where the coefficients  $a_{ij}$  are related to the initial state of the qubit (see below). Each operator  $\rho_{ij}(t)$  acts on

the Hilbert space of the harmonic oscillator. In this way, Eq. (1) separates into independent evolution equations for each of these operators. With  $H_\pm = H_{\text{osc}} \pm g \hat{x}$ , we find

$$i \frac{d\rho_{00}}{dt} = [H_+, \rho_{00}] + \mathcal{L}[\rho_{00}], \quad (7)$$

$$i \frac{d\rho_{11}}{dt} = [H_-, \rho_{11}] + \mathcal{L}[\rho_{11}], \quad (8)$$

$$i \frac{d\rho_{01}}{dt} = (H_+ \rho_{01} - \rho_{01} H_-) + \frac{\Delta}{2} \rho_{01} + \mathcal{L}[\rho_{01}]. \quad (9)$$

We assume the initial state to be a product state of the form

$$\rho(0) = \begin{pmatrix} a_{00} & a_{01} \\ a_{10} & a_{11} \end{pmatrix} \otimes \rho_{\text{osc}}. \quad (10)$$

In the evolution equations (7-9), the coupling term between qubit and oscillator appears as a perturbation to the dynamics of the oscillator mode. This makes it possible to study its fidelity or (quantum Loschmidt echo) [4]. Without dissipation and for a pure initial state, this fidelity  $F(t)$  can be obtained from both, the diagonal and the off-diagonal blocks [1, 46]. From the diagonal blocks, we obtain

$$\begin{aligned} \rho_{00}(t) &= |\psi_+(t)\rangle\langle\psi_+(t)| : \psi_+(t) = e^{-iH_+t} |\psi(0)\rangle, \\ \rho_{11}(t) &= |\psi_-(t)\rangle\langle\psi_-(t)| : \psi_-(t) = e^{-iH_-t} |\psi(0)\rangle, \end{aligned} \quad (11)$$

where  $|\psi_+(0)\rangle = |\psi_-(0)\rangle = |\psi(0)\rangle$  is the pure initial state of the oscillator mode. From this, we obtain the quantum fidelity as

$$F(t) = \text{Tr}[\rho_{00}(t) \rho_{11}(t)] = |\langle\psi_+(t)|\psi_-(t)\rangle|^2. \quad (12)$$

From the off-diagonal block, we get

$$\begin{aligned} \rho_{01}(t) &= e^{i\Delta t} e^{-iH_-t} \rho_{01}(0) e^{iH_+t} \\ &= e^{i\Delta t} |\psi_-(t)\rangle\langle\psi_+(t)|, \end{aligned} \quad (13)$$

while  $\rho_{10}(t) = \rho_{01}(t)^\dagger$ . This allows us to write

$$F(t) = \text{Tr}[\rho_{01}(t) \rho_{10}(t)]. \quad (14)$$

If we include dissipation and/or mixed initial states, then the strict equivalence between the Eqs. (12) and (14) breaks down. In that case, the operators  $\rho_{00}(t)$  and  $\rho_{11}(t)$  become density matrices, which are the solutions of a quantum master equation of Lindblad from [47–49]. Concerning the diagonal blocks, we use a standard generalization of fidelity to the case of mixed quantum states, which is due to Uhlmann [40] (mathematical definition) and Jozsa [41]. Thus we define

$$F_{\text{UJ}}(t) = \text{Tr}(\rho_{00}(t)^{1/4} \rho_{11}(t)^{1/2} \rho_{00}(t)^{1/4})^2. \quad (15)$$

Concerning the non-diagonal blocks, we interpret Eq. (14) as a different measure for (the loss of) fidelity in an open quantum system, and denote that quantity

$$F_{\text{gen}}(t) = \text{Tr}[\rho_{01}(t) \rho_{10}(t)] = |\text{Tr}[\rho_{01}(t)]|^2. \quad (16)$$

as the generalized fidelity [17, 50].

There are important conceptual differences between  $F_{\text{UJ}}(t)$  and  $F_{\text{gen}}(t)$ :  $F_{\text{UJ}}(t)$  can be used to quantify the similarity of mixed quantum states, it is not necessary that these are states evolving under certain evolution equations. By contrast,  $F_{\text{gen}}(t)$  requires to specify these evolution equations. It also requires that these are of Lindblad form and differ in the Hamiltonian part only. Furthermore, in a typical case, the master equations for the two diagonal blocks guide any initial state to the same equilibrium state. Therefore,  $F_{\text{UJ}}(t)$  will typically increase towards one at the end. By contrast,  $F_{\text{gen}}(t)$  will often drop to zero.

### B. Wigner and chord function description

The solutions derived here are carried out by employing the chord function description [51–53]. The chord function (or the characteristic Wigner function) is defined as the Fourier transform of the Wigner function [54]. In what follows we review some of their properties.

*a. Wigner function* We start with the position representation of an operator  $\hat{A}$ . If this operator has a matrix representation with respect to some orthonormal basis  $\{\varphi_j\}_{j \in \mathbb{N}}$ ,

$$\langle x | \hat{A} | x' \rangle = \sum_{ij} A_{ij} \langle x | \varphi_i \rangle \langle \varphi_j | x' \rangle = \sum_{ij} A_{ij} \varphi_i(x) \varphi_j(x')^*, \quad (17)$$

where  $\langle x | \varphi_j \rangle$  is the Dirac notation for the familiar wave function representation  $\varphi_j(x)$ . Then, we may define the Wigner function of a given collection of quantum states described by the density matrix  $\varrho$  as

$$W_\varrho(q, p) = \frac{1}{2\pi} \int dy e^{-ipy} \langle q + y/2 | \varrho | q - y/2 \rangle. \quad (18)$$

This is also called the Weyl symbol of the density matrix  $\varrho$ . Now, the expectation value of any observable  $\hat{A}$  can be calculated as a phase space integral:

$$\text{tr}[\hat{A} \varrho] = \iint dp dq W_A(q, p) W_\varrho(q, p), \quad (19)$$

where  $W_A(q, p)$  is the Weyl symbol [55, 56] of the observable  $\hat{A}$ . In order to transfer the evolution equations (7-9) into phase space, we need to know how multiplication with position and momentum operators from left and right is translated to the Wigner function representation. It is easily verified [57]

$$\begin{aligned} \hat{q} \varrho &\mapsto \left(q - \frac{i}{2} \partial_p\right) W_\varrho, & \hat{p} \varrho &\mapsto \left(p + \frac{i}{2} \partial_q\right) W_\varrho \\ \varrho \hat{q} &\mapsto \left(q + \frac{i}{2} \partial_p\right) W_\varrho, & \varrho \hat{p} &\mapsto \left(p - \frac{i}{2} \partial_q\right) W_\varrho. \end{aligned} \quad (20)$$

*b. Chord function (characteristic Wigner function)* The chord function [51–53] is defined as the Fourier transform of the Wigner function [54, 58]

$$\begin{aligned} w(k, s) &= \iint dp dq e^{iqk + isp} W_\varrho(q, p) \\ &= \int dq e^{iqk} \langle q + s/2 | \varrho | q - s/2 \rangle. \end{aligned} \quad (21)$$

Due to this relation, Eq. (20) can be readily translated into similar expressions for the application of position and momentum operators to the chord function (for later convenience, higher powers of  $\hat{x}$  and  $\hat{p}$  are included):

$$\hat{x}^n \hat{p}^m \varrho \mapsto \left(\frac{s}{2} - i\partial_k\right)^n \left(\frac{-k}{2} - i\partial_s\right)^m w(k, s) \quad (22)$$

$$\varrho \hat{x}^n \hat{p}^m \mapsto \left(\frac{-s}{2} - i\partial_k\right)^n \left(\frac{k}{2} - i\partial_s\right)^m w(k, s) \quad (23)$$

$$\hat{x}^n \varrho \hat{p}^m \mapsto \left(\frac{s}{2} - i\partial_k\right)^n \left(\frac{k}{2} - i\partial_s\right)^m w(k, s) \quad (24)$$

$$\hat{p}^m \varrho \hat{x}^n \mapsto \left(\frac{-s}{2} - i\partial_k\right)^n \left(\frac{-k}{2} - i\partial_s\right)^m w(k, s). \quad (25)$$

This also allows to obtain explicit expressions for the  $n$ -th order moments of products of position and momentum operators, by taking the appropriate partial derivatives at the origin of the coordinate system:

$$\begin{aligned} \langle \hat{x}^n \rangle &= (-i\partial_k)^n w|_{k,s=0}, & \langle \hat{p}^n \rangle &= (-i\partial_s)^n w|_{k,s=0} \\ \frac{\langle \hat{x}^n \hat{p}^m \rangle + \langle \hat{p}^m \hat{x}^n \rangle}{2} &= (-i)^{n+m} \partial_k^n \partial_s^m w|_{k,s=0}. \end{aligned} \quad (26)$$

These equations may explain the name “characteristic Wigner function”.

In the next section, we use the properties presented here, to transfer the evolution equations (7-9) to partial differential equations for the corresponding chord functions, which are then solved analytically. In order to compute the Uhlmann-Josza fidelity, we use a result from Isar [39]. For calculating the generalized fidelity, we compute the trace of  $\varrho_{01}(t)$ . In the chord function representations, this simply means that the respective chord function must be evaluated at  $k, s = 0$ . This follows from Eqs. (19) and (21).

### III. ANALYTIC SOLUTION

In the chord function representation, the equations (7-9) for the block matrices  $\varrho_{ij}(t)$  defined in Eq. (6) become the following set of partial differential equations:

$$\hat{L}_d w_{00} = -\left(ig s + \frac{\gamma_+}{2}(k^2 + s^2)\right) w_{00} \quad (27)$$

$$\hat{L}_{nd} w_{01} = -\left(i\Delta + \frac{\gamma_+}{2}(k^2 + s^2)\right) w_{01}, \quad (28)$$

where  $w_{00}$  ( $w_{01}$ ) is the chord function representation of  $\varrho_{00}$  ( $\varrho_{01}$ ) from Eqs. (7-9),  $\gamma_+ = \kappa(2\bar{n} + 1)$ , and

$$\hat{L}_d = \partial_\tau + (s + \kappa k)\partial_k - (k - \kappa s)\partial_s \quad (29)$$

$$\hat{L}_{nd} = \partial_\tau + (s + \kappa k + 2g)\partial_k - (k - \kappa s)\partial_s. \quad (30)$$

These differential equations can be solved analytically, using the method of characteristics (see the appendix). Thereby we find for  $w_{00}$ :

$$w_{00}(\vec{r}, t) = w_{\text{osc}}(\mathbf{R}(-t)\vec{r}) \times \exp\left(-\frac{i}{2}\vec{d}(t) \cdot \vec{r} - \frac{\alpha(t)}{2}|\vec{r}|^2\right), \quad (31)$$

where the vector  $\vec{r} = (k, s)^T$  collects the two independent variables of the chord function representation, and  $w_{\text{osc}}(\vec{r})$  represents the initial state of the oscillator in the chord function representation. Furthermore, we have introduced the following quantities:

$$\mathbf{R}(t) = e^{\kappa t} \begin{pmatrix} \cos t & \sin t \\ -\sin t & \cos t \end{pmatrix}, \quad (32)$$

$$\vec{d}(t) = \begin{pmatrix} d_1(t) \\ d_2(t) \end{pmatrix}, \quad d_j(t) = 2g \int_0^t d\tau R_{2j}(-\tau), \quad (33)$$

where  $R_{21}$  and  $R_{22}$  are the respective matrix elements of  $\mathbf{R}(\tau)$ , and  $\alpha(t) = (\bar{n} + 1/2)(1 - e^{-2\kappa t})$ . The solution for  $w_{11}(\vec{r}, t)$  can be obtained from  $w_{00}(\vec{r}, t)$  by simply changing the sign of  $g$ :

$$w_{11}(\vec{r}, t) = w_{\text{osc}}(\mathbf{R}(-t)\vec{r}) \times \exp\left(\frac{i}{2}\vec{d}(t) \cdot \vec{r} - \frac{\alpha(t)}{2}|\vec{r}|^2\right). \quad (34)$$

From the Wigner function representations, calculated below, it can be seen that  $\pm\vec{d}(t)/2$  points at the position of the Gaussian state, as it evolves in phase space under the Hamiltonian  $H_{\pm}$ . In other words, its components are the expectation values of position and momentum as they evolve in time.

As far as the initial conditions are concerned, Eq. (10), we restrict ourselves to thermal or coherent Gaussian states for the oscillator. In the chord function representation; these states have the generic form:

$$w_{\text{osc}}(\vec{r}) = \exp\left(i\vec{x}_o \cdot \vec{r} - \frac{1}{2}\vec{r}^T \boldsymbol{\sigma}_o \vec{r}\right), \quad (35)$$

where the vector  $\vec{x}_o = (x_o, p_o)^T$  contains the expectation values of position and momentum, and  $\boldsymbol{\sigma}_o$  is the corresponding covariance matrix. The uncertainty principle requires that  $\det(\boldsymbol{\sigma}_o) \geq 1/4$ .

The chord function representation  $w_{01}$  of the non-diagonal block can be obtained in a similar manner (see App. A 2). The result reads

$$w_{01}(\vec{r}, t) = w_{\text{osc}}(\mathbf{R}(-t)\vec{r} + \vec{\eta}(-t)) \times \exp\left(-\frac{\alpha(t)}{2}|\vec{r}|^2 - \frac{\gamma_+}{2}\vec{\Gamma}(t) \cdot \vec{r}\right) \quad (36)$$

$$\times \exp\left(-i\Delta t - \frac{\gamma_+}{2}\delta(t)\right), \quad (37)$$

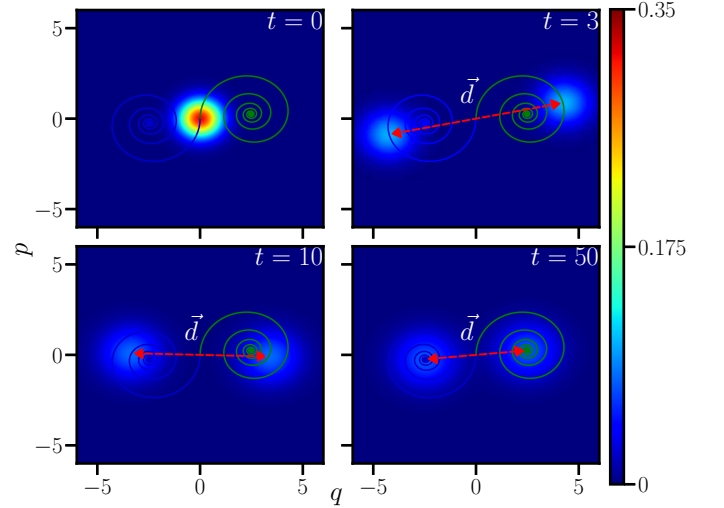


FIG. 1. False color plots of the Wigner function representation of the reduced harmonic oscillator state, for an initial product state  $\varrho(0)$ , Eq. (10), built from a symmetric superposition with  $a_{ij} = 1/2$  for the qubit and the harmonic oscillator ground state. The qubit-oscillator coupling is chosen as  $g = 2.5$ , the dissipation rate as  $\kappa = 0.1$ , and the dimensionless temperature as  $D = 1$ ; see Eq. (5). The thin solid lines (green and blue) show the classical trajectories under the Hamiltonians  $H_+$  and  $H_-$ , respectively. The red two-sided arrow indicates the vector  $\vec{d}$ , introduced in Eq.(33). The different panels, show the Wigner function and the vector  $\vec{d}$  at different dimensionless times,  $t = 0, 3, 10, 50$ .

where we have introduced the following quantities:

$$\vec{\eta}(t) = \frac{2g}{1 + \kappa^2} (\mathbf{R}(-t) - \mathbb{1}) \begin{pmatrix} \kappa \\ 1 \end{pmatrix} = - \begin{pmatrix} d_2(t) \\ d_1(t) \end{pmatrix} \quad (38)$$

$$\delta(t) = \int_0^t dt' |\vec{\eta}(t')|^2 = \int_0^t dt' d(t')^2 \quad (39)$$

$$\vec{\Gamma}(t) = 2 \int_0^t dt' \mathbf{R}^T(-t') \vec{\eta}(t'), \quad (40)$$

where  $d(t) = |\vec{d}(t)| = |\vec{\eta}(t)|$ . Due to this, the function  $\delta(t)$  appearing in the solution for the non-diagonal term of the qubit is determined by the distance between the two Gaussians in phase space.

## A. Oscillator dynamics

In order to illustrate the general behavior of our system, we discuss its reduced dynamics at very strong qubit-oscillator coupling,  $g = 2.5$ . As initial state we chose a product state of the form given in Eq. (10) with  $a_{ij} = 1/2$  and  $\varrho_{\text{osc}}$  being the oscillator ground state. In the present section, we consider the Wigner function of the reduced state after tracing over the qubit, in the next section III B, we discuss the reduced state of the qubit.

For the Wigner function of the reduced oscillator state,



we find

$$W(\vec{x}, t) = a_{00} W_+(\vec{x}, t) + a_{11} W_-(\vec{x}, t), \quad (41)$$

where the Wigner functions  $W_{\pm}(\vec{x}, t)$  have the following form:

$$W_{\pm}(\vec{x}, t) = \frac{1}{2\pi\sqrt{\det\sigma(t)}} e^{-\frac{1}{2}(\vec{x}-\vec{x}_o^{\pm}(t))^T \sigma(t)^{-1} (\vec{x}-\vec{x}_o^{\pm}(t))}. \quad (42)$$

The Wigner functions conserve their Gaussian shape, while their covariance matrix

$$\sigma(t) = \alpha(t) \mathbb{1} + \mathbf{R}^T(-t) \sigma_o \mathbf{R}(-t) \quad (43)$$

becomes time dependent. Note the following definitions:  $\vec{x} = (q, p)^T$  and  $\vec{x}_o^{\pm}(t) = \mathbf{R}^T(-t) \vec{x}_o \pm \vec{d}(t)/2$ .

In Fig. 1 we plot  $W(\vec{x}, t)$  from Eq. (41) at different instances in time. The figure shows how the interaction with the qubit results in the splitting of the initial Gaussian wave packet into two Gaussians, following the classical trajectories of  $H_+$  and  $H_-$ , respectively. For large times (note that the oscillator period is  $T_{\text{osc}} = 2\pi$ ), one obtains a stationary state, where the two Gaussian wave packets are located on the  $q$ -axis, each packet in the minimum of the corresponding  $g$ -perturbed Hamiltonian. We will see, that the relative vector  $\vec{d}(t)$  between the two wave packets determines the fidelity measures, to be discussed below.

### B. Qubit dynamics

The reduced state of the qubit is obtained by tracing Eq. (6) over the oscillator degrees of freedom. This corresponds to evaluating the solutions given in Eqs. (31) and (37), at the origin  $\vec{r} = 0$ . Since  $\varrho_{00}(t)$  and  $\varrho_{11}(t)$  are valid density matrices for all times, the diagonal elements of the qubit state remain constant. In contrast to that the non-diagonal element does depend on time via

$$\text{Tr}[\varrho_{01}(t)] = w_{\text{osc}}(\vec{\eta}(-t)) \exp\left(-i\Delta t - \frac{\gamma_+}{2} \delta(t)\right), \quad (44)$$

$$\text{where } \delta(t) = \int_0^t dt' d^2(t').$$

## IV. FIDELITY MEASURES

### A. Generalized fidelity

Within the chord function description one can directly use Eq. (44) to obtain an explicit expression for the generalized fidelity, Eq. (16). In this way, we obtain

$$F_{\text{gen}}(t) = |w_{\text{osc}}(\vec{\eta}(t))|^2 \exp(-\gamma_+ \delta(t)). \quad (45)$$

In the case of a general initial Gaussian state as described in Eq. (35), the generalized fidelity takes the following form:

$$F_{\text{gen}}(t) = \exp(-\vec{\eta}^T(t) \sigma_o \vec{\eta}(t) - \gamma_+ \delta(t)). \quad (46)$$

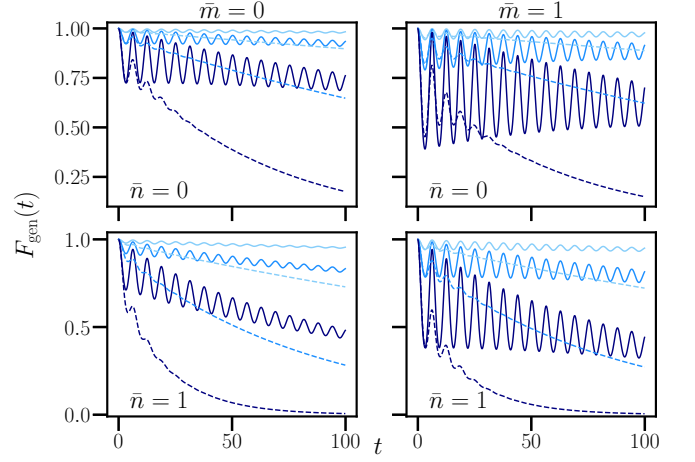


FIG. 2. The generalized fidelity  $F_{\text{gen}}(t)$  as a function of time, for different couplings between qubit and oscillator:  $g = 0.05$  (light blue),  $0.1$  (blue),  $0.2$  (dark blue), and different environment coupling:  $\kappa = 0.01$  (solid lines), and  $0.1$  (dashed lines). The four panels show the results for different thermal initial states (characterized by  $\bar{m}$ ) and different temperatures of the environment (characterized by  $\bar{n}$ ), as indicated on each panel.

In the rest of the paper, we concentrate on initial thermal states, where  $\sigma_o = M \mathbb{1}$  with  $M = \bar{m} + 1/2$ , and  $x_o = p_o = 0$ ; see Eq. (35). In that case, the generalized fidelity becomes

$$F_{\text{gen}}(t) = \exp[-M d(t)^2 - \gamma_+ \delta(t)]. \quad (47)$$

Here,  $\gamma_+ = N\kappa$ , with  $N = (2\bar{n} + 1)$  as defined below Eq. (28). The function  $d(t)$  is positive, with decaying oscillations, which tends to a constant in the long time limit. Correspondingly,  $\delta(t)$  is increasing monotonously, becoming approximately linear at sufficiently long times or when averaged over several oscillator periods. The expression in Eq. (47) simplifies further in the limit of vanishing coupling,  $\kappa \rightarrow 0$ , where

$$F_{\text{gen}}(t) \rightarrow \exp[-8M g^2 (1 - \cos t)]. \quad (48)$$

Note that for  $M = 1/2$  only, the expression reduces to the standard fidelity of a pure quantum state under the perturbation of a unitary evolution, as described in Eq. (12).

Figure 2 shows the generalized fidelity for increasing values of the coupling strength  $g$  (from light to dark blue), different environment couplings  $\kappa$ , different temperatures of the initial states and the environment. The initial states are of the form given in Eq. (35) with  $x_o = p_o = 0$  and  $\sigma_o = (\bar{m} + 1/2)\mathbb{1}$ , while the temperature of the environment is characterized by the corresponding average number of excited modes  $\bar{n}$ , as defined in Eq. (5).

In all cases, the generalized fidelity ultimately tends to zero in the large time limit. Since  $d(t) \rightarrow 2g/\sqrt{1 + \kappa^2}$  in the limit of large times, the slowest possible decay rate is given by

$$\lim_{t \rightarrow \infty} t^{-1} \gamma_+ \delta(t) = \frac{\kappa}{1 + \kappa^2} (2\bar{n} + 1) 4g^2, \quad (49)$$

which can be easily calculated from Eq. (33).

The exponent in Eq. (47) consists of two terms. The first term alone would yield decaying oscillations, in such a way that  $F_{\text{gen}}(t)$  tends to one. The initial amplitude of these oscillations is determined by  $M$ , their damping however scales with  $\kappa$ . The second term alone would yield a monotonously decaying function, with a decay rate scaling with  $N\kappa g^2$ . This behavior is clearly reflected in the four panels of Fig. 2, even though there are cases where the time range considered is too small to observe the complete decay.

### B. Uhlmann-Josza fidelity

In Ref. [39], the author calculates the Uhlmann-Josza fidelity for two arbitrary Gaussian states, *i.e.* states where the position representation, Eq. (17), of their density matrix is the exponential function of a quadratic polynomial in the two variables. In that case, the fidelity is determined completely by the first and second order moments of the position and momentum operators. In this sense, the chord function in Eq. (35) and the corresponding Wigner function

$$W_{\text{osc}}(\vec{x}) = \frac{1}{2\pi \sqrt{\det(\sigma_o)}} e^{-\frac{1}{2}(\vec{x}-\vec{x}_o)^T \sigma_o^{-1}(\vec{x}-\vec{x}_o)},$$

represent such a general Gaussian state. In that case, the first order moments are given by  $\vec{x}_o = (x_o, p_o)^T$ , while the second order moments are collected in the covariance matrix  $\sigma_o$

$$\sigma_o = \begin{pmatrix} \sigma_{11} & \sigma_{12} \\ \sigma_{12} & \sigma_{22} \end{pmatrix}, \quad \begin{aligned} \sigma_{11} &= \langle \hat{x}^2 \rangle - \langle \hat{x} \rangle^2 \\ \sigma_{22} &= \langle \hat{p}^2 \rangle - \langle \hat{p} \rangle^2 \\ \sigma_{12} &= \frac{1}{2} \langle \hat{x}\hat{p} + \hat{p}\hat{x} \rangle - \langle \hat{x} \rangle \langle \hat{p} \rangle \end{aligned} \quad (50)$$

Assume  $\varrho_1$  and  $\varrho_2$  are two general Gaussian states, with first order moments  $\vec{x}_1$  and  $\vec{x}_2$ , as well as covariance matrices  $\sigma_1$  and  $\sigma_2$ , respectively. Then it is shown in Ref. [39] that the Uhlmann-Josza fidelity, defined in Eq. (15), can be written as

$$F_{\text{UJ}}(\varrho_1, \varrho_2) = \frac{1}{\sqrt{\mu+4\nu} - \sqrt{4\nu}} e^{-\frac{1}{2} \vec{d}^T (\sigma_1 + \sigma_2)^{-1} \vec{d}}, \quad (51)$$

where  $\mu = \det(\sigma_1 + \sigma_2)$ ,  $\nu = [\det(\sigma_1) - 1/4][\det(\sigma_2) - 1/4]$  and  $\vec{d} = \vec{x}_2 - \vec{x}_1$ .

In order to apply Isar's result, Eq. (51), to the density matrices  $\varrho_{00}(t)$  and  $\varrho_{11}(t)$ , as prescribed in Eq. (15), we note that the vector  $\vec{d}$  must be chosen as  $\vec{d}(t)$  from Eq. (33), since it is exactly the distance vector between the first order moments of  $\varrho_{00}(t)$  and  $\varrho_{11}(t)$  in phase space. The corresponding covariance matrices are the same and equal to  $\sigma(t)$ , as given in Eq. (43). Therefore, we find

$$\mu = 4 \det[\sigma(t)], \quad 4\nu = \frac{[4 \det[\sigma(t)] - 1]^2}{4},$$

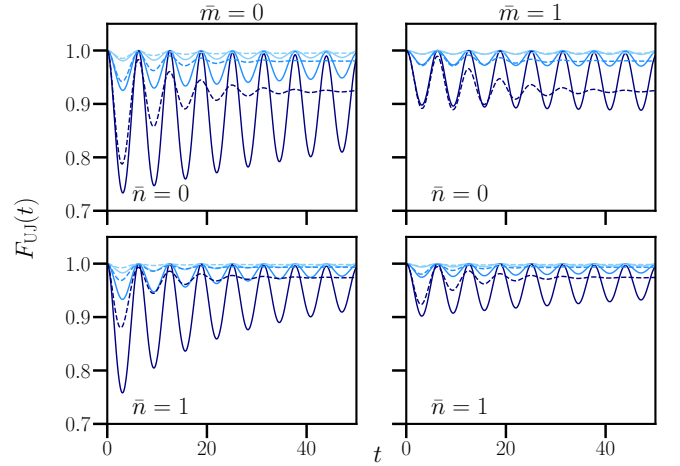


FIG. 3. The Uhlmann-Josza fidelity  $F_{\text{UJ}}(t)$  as a function of time, for different couplings between qubit and oscillator:  $g = 0.05$  (light blue),  $0.1$  (blue),  $0.2$  (dark blue), and different environment coupling  $\kappa = 0.01$  (solid lines), and  $0.1$  (dashed lines). The four panels show the results for different thermal initial states (characterized by  $\bar{m}$ ) and different temperatures of the environment (characterized by  $\bar{n}$ ), as indicated on each panel.

which yields  $\sqrt{\mu+4\nu} = 2 \det[\sigma(t)] + 1/2$  and thereby  $\sqrt{\mu+4\nu} - \sqrt{4\nu} = 1$ . Thus, we are left with

$$F_{\text{UJ}}(t) = \exp \left( -\frac{1}{4} \vec{d}^T(t) \sigma^{-1}(t) \vec{d}(t) \right), \quad (52)$$

where  $\sigma(t)$ , given in Eq. (43), simplifies to

$$\sigma(t) = \alpha(t) \mathbb{1} + e^{-2\kappa t} M \mathbb{1} = [N + (M - N) e^{-2\kappa t}] \mathbb{1},$$

in the case of a thermal initial state with  $\sigma_0 = M \mathbb{1}$ . In that latter case,

$$F_{\text{UJ}}(t) = \exp \left( -\frac{1}{4} \frac{d(t)^2}{N + (M - N) e^{-2\kappa t}} \right). \quad (53)$$

Figure 3 shows the time evolution of the Uhlmann-Josza fidelity in the same conditions and with the same line types and color codings as in the case of the generalized fidelity shown in Fig. 2. The most striking difference between the two fidelities can be observed in their behavior at long times. While the generalized fidelity ultimately decays to zero in all case, the Uhlmann-Josza fidelity tends to the constant

$$\lim_{t \rightarrow \infty} F_{\text{UJ}}(t) = \exp \left( \frac{-g^2}{N(1 + \kappa^2)} \right) \quad (54)$$

[see Eq. (55), below]. Both quantities strongly depend on  $d(t)$ , and by consequence show very similar oscillatory behavior with a period similar to the fundamental oscillator period.

### C. Connecting quantities

In this section, we discuss the possibility to use the qubit as a probe system for extracting information about the evolution of the oscillator in contact with a heat bath. Evidently, all the information extractable from the qubit must be contained in the generalized fidelity  $F_{\text{gen}}(t)$ . We limit ourselves to initial thermal states of the oscillator – not necessarily in equilibrium with the heat bath.

(i) In a first approach, we simply take advantage of the fact that the behavior of the system is known analytically. In principle, it is therefore sufficient to determine all relevant parameters of the system in order to determine its dynamics. In our particular case, these parameters are:  $g$  the coupling between qubit and oscillator,  $\kappa$  the coupling between the oscillator and the heat bath, and finally  $M$  and  $N$  which characterize the temperature of the initial state and the heat bath respectively. Calculating the logarithmic derivative of the generalized fidelity, we find the following analytic expression:

$$H(t) = -\frac{d}{dt} \ln [F_{\text{gen}}(t)] = M \frac{d}{dt} d^2(t) + 2\kappa N d^2(t) ,$$

$$d^2(t) = \frac{4g^2}{1+\kappa^2} (e^{-2\kappa t} - 2e^{-\kappa t} \cos t + 1) . \quad (55)$$

Thus, in principle, it seems that the function  $H(t)$  depends on all four parameters in an independent way. Therefore, a non-linear parameter fit may be used to estimate their values.

(ii) As an alternative, we could try to determine the function  $d^2(t)$  directly, using the fact that it only depends on  $\kappa$  and  $g$  but not its particular form. This is possible by measuring  $F_{\text{gen}}(t)$  for two initial states of different temperatures,  $M_1$  and  $M_2$  (assuming these are known a priori). In that case, one obtains:

$$\frac{\ln[F_{\text{gen}}^{(M_1)}(t)] - \ln[F_{\text{gen}}^{(M_2)}(t)]}{M_2 - M_1} = d^2(t) . \quad (56)$$

Now, we can estimate  $g$  and  $\kappa$  separately from the behavior of  $d^2(t)$ . Then, in a second step, we estimate the temperature  $N$  of the heat bath from the identity

$$\frac{M_2 \ln[F_{\text{gen}}^{(M_1)}(t)] - M_1 \ln[F_{\text{gen}}^{(M_2)}(t)]}{M_1 - M_2} = \kappa N \delta(t) . \quad (57)$$

This method may be more robust as the first one, since we do not estimate so many parameters from one single function.

*Uhlmann-Josza fidelity* Once, the function  $d^2(t)$  is known, together with the parameters  $N, M$  and  $\kappa$ , we can reconstruct the Uhlmann-Josza fidelity with the help of Eq. (53). At the moment, it is still an open question, whether this or a similar relation may hold in more

general cases also. These cases may include: 1. different initial states for instance coherent states away from the equilibrium point, 2. cat states – i.e. superpositions of coherent states, etc.

*Purities of the reduced states* As it turns out, the purities of the reduced states, of the qubit but also of the oscillator, can be related in a very similar manner to the respective quantum fidelities. In the case of the qubit reduced state, this is fairly obvious:

$$P_q(t) = a_{00}^2 + a_{11}^2 + 2|a_{01}|^2 F_{\text{gen}}^{(M)}(t) . \quad (58)$$

In the case of the oscillator reduced state, this follows from the fact that

$$P_{\text{osc}}(t) = 2\pi \iint dp dq W^2(\vec{x}, t) ,$$

with  $W(\vec{x}, t)$  given by (41). In that case,

$$P_{\text{osc}}(t) = \frac{a_{00}^2 + a_{11}^2 + 2a_{00}a_{11}F_{\text{UJ}}^{(M)}(t)}{2\sqrt{\det \sigma(t)}} . \quad (59)$$

### V. CONCLUSIONS

We considered an open quantum system consisting of a harmonic oscillator being coupled to a finite-temperature heat bath, equipped with an additional two-level system (qubit). This qubit is coupled to the oscillator via dephasing coupling, and serves as a probe for the dynamics of the system. The quantum master equation, which describes the evolution of the whole system, can be solved analytically, using the Fourier transform of the Wigner function, the so called “chord function”.

Provided the two-level probe is initially prepared in a superposition state, the loss of coherence over time provides sufficient information in order to determine the complete dynamics of the dissipative oscillator. In other words, based on the decoherence function, we can estimate all relevant parameters of the dynamics: the temperature of the heat bath, that of the initial state (*e.g.* in the case we are interested in a temperature quench), the coupling strength to the bath as well as that of the probe.

The present setup, provides the rare opportunity to study analytically the behavior of the Uhlmann-Josza fidelity between mixed states subject to different evolutions in time. We use this to investigate similarities and differences between the decoherence function, which is almost identical to the generalized fidelity as introduced in Ref. [17], and the standard Uhlmann-Josza fidelity.

So far, we restricted ourselves to thermal initial states. In that case, the coupling to the qubit gives rise to two different evolutions governed by separated harmonic potentials. It would be interesting to study more general initial states, such as displaced Gaussian states, similar to those which have been analyzed in the Jaynes-Cummings

model of cavity QED [59], or cat states; or one could even consider Schrödinger cat states as initial states. That would allow us to investigate the relation between generalized and Uhlmann-Josza fidelity from a more general perspective.

In addition, we may find interesting applications in the area of quantum thermodynamics. For instance, we may realize Carnot cycles with the harmonic oscillator at finite times, and monitor the evolving state with the help of the coupled qubit. Since the coupling between qubit and oscillator is of dephasing type, the systems cannot interchange energy thus one can observe the evolution of the thermodynamic system without affecting its thermodynamic properties. A possible experimental realization could be build from two-level atoms in an harmonic trap, where the dephasing coupling and the measurement of the decoherence function is easy to achieve [1, 46, 60].

### Appendix A: Derivation of the solutions of the generalized master equations

By using the notation  $\langle i|\varrho|j\rangle = \varrho_{ij}$  for  $i, j = 0, 1$  represent the projection of the system into the different states of the qubit. The matrix elements master equations may be written as:

$$i \frac{d\varrho_{00}}{dt} = [H_{\text{osc}}, \varrho_{00}] + g[\hat{x}, \varrho_{00}] + i\mathcal{L}[\varrho_{00}] \quad (\text{A1})$$

$$i \frac{d\varrho_{01}}{dt} = [H_{\text{osc}}, \varrho_{01}] + \{\Delta/2 + g\hat{x}, \varrho_{01}\} + i\mathcal{L}[\varrho_{01}] \quad (\text{A2})$$

where  $\mathcal{L}[\varrho_{ij}]$  is given by (4). The solution to the matrix elements master equations can be more easily carried out by employing the chord function description. By doing the transformations, matrix elements master equations can be written as a set of partial differential equations:

$$\hat{L}_d w_{00} = -\left(ig s + \frac{\gamma_+}{2}(k^2 + s^2)\right) w_{00} \quad (\text{A3})$$

$$\hat{L}_{nd} w_{01} = -\left(i\Delta + \frac{\gamma_+}{2}(k^2 + s^2)\right) w_{01} \quad (\text{A4})$$

where we have defined  $\gamma_+ = 2\kappa(\bar{n} + 1/2)$ , and

$$\hat{L}_d = \partial_t + (s + \kappa k)\partial_k - (k - \kappa s)\partial_s \quad (\text{A5})$$

$$\hat{L}_{nd} = \partial_t + (s + \kappa k + 2g)\partial_k - (k - \kappa s)\partial_s \quad (\text{A6})$$

#### 1. Diagonal element $w_{00}$

For equation (A3) one can write down the set of parametric differential equations in the following form:

$$\frac{dk}{dt} = s + \kappa k, \quad \frac{ds}{dt} = -k + \kappa s \quad (\text{A7})$$

$$\frac{dw_{00}}{dt} = -\left[ig s + \frac{\gamma_+}{2}(k^2 + s^2)\right] w_{00}, \quad (\text{A8})$$

and by coupling the first two equations (A7), we can write down a second order ordinary differential equation for  $k$ :

$$\ddot{k} - \beta\dot{k} + \omega^2 k = 0, \quad (\text{A9})$$

where  $\omega^2 = 1 + \kappa^2$ . The solution of equation (A9) may be written as:

$$k(\tau) = e^{\kappa\tau} (a_1 \sin t + a_2 \cos t) \quad (\text{A10})$$

where  $a_1$  and  $a_2$  are the characteristic curves which remain constant for all time. The variable  $s(t)$  may be obtained through first equation of (A7),  $s = \dot{k} - \kappa k$  yielding:

$$s(t) = e^{\kappa t} (a_1 \cos t - a_2 \sin t). \quad (\text{A11})$$

For these type of linear differential equations, one can always define the fundamental matrix which maps any point  $(k(t'), s(t'))$  at the time  $t'$ , along the characteristics to any other point  $(k(t), s(t))$  at time  $t$  as  $\vec{r}(t) = \mathbf{R}(t - t')\vec{r}(t')$ . For time invariant systems where the parameter are no time dependent, the fundamental matrix has a closed form. In the present case, this one has the following form:

$$\mathbf{R}(t) = e^{\kappa t} \begin{pmatrix} \cos t & \sin t \\ -\sin t & \cos t \end{pmatrix}. \quad (\text{A12})$$

This fundamental matrix has the property that it only depends of the difference of the initial and final time and posses group properties in the sense that  $\mathbf{R}(t_2 - t_0) = \mathbf{R}(t_2 - t_1)\mathbf{R}(t_1 - t_0)$  for all times except in the limit where  $t \rightarrow \pm\infty$  for which it becomes singular. At any other time, the fundamental matrix always fulfills  $\mathbf{R}(-t) = \mathbf{R}^{-1}(t)$ . The integration of (A3) is done as follows;

$$\int_{w_{00}(0)}^{w_{00}(t)} \frac{dw_{00}}{w_{00}} = -ig \int_0^t dt' s(t') - \frac{\gamma_+}{2} \int_0^t dt' (k^2(t') + s^2(t')). \quad (\text{A13})$$

Within the fundamental matrix, the integration over the right hand side can be calculated by using the fact that

$$\vec{r}(t') = \mathbf{R}(t' - t)\vec{r}(t), \quad (\text{A14})$$

thus, we can write down an explicitly expression for the evolution of this chord function matrix element as:

$$w_{00}(\vec{r}, t) = w_{00}(\mathbf{R}(-t)\vec{r}, \tau) \exp\left(-\frac{i}{2}\vec{d}(t) \cdot \vec{r} - \frac{\gamma_+}{2}\alpha(t)|\vec{r}|^2\right) \quad (\text{A15})$$

where  $\alpha(t)$  is given by

$$\alpha(t) = \int_0^t dt' [R_{11}^2(-t') + R_{12}^2(-t')] = \frac{1 - e^{-\kappa t}}{\kappa}, \quad (\text{A16})$$

and  $\vec{d}(t) = (d_1(t), d_2(t))^T$  where its components have the following form ( $j = 1, 2$ ):

$$d_j(t) = 2g \int_0^t dt' R_{2j}(-t'). \quad (\text{A17})$$

where  $R_{21}$  and  $R_{22}$  are matrix elements of the map described in Eq. (A12).



## 2. Non-diagonal element $w_{01}$

For the non-diagonal element master equation (A4), its parametric form is given by:

$$\frac{dk}{dt} = s + \kappa k + 2g, \quad \frac{ds}{dt} = -k + \kappa s, \quad (\text{A18})$$

$$\frac{dw_{01}}{dt} = -\left(i\Delta + \frac{\gamma_+}{2}(k^2 + s^2)\right) w_{01}. \quad (\text{A19})$$

As before, one can write down a second order ordinary differential equation for  $k$  by coupling the first two equations (A18) yielding:

$$\ddot{k} - 2\kappa\dot{k} + (1 + \kappa^2)k = -2\kappa g, \quad (\text{A20})$$

The solution of equation (A20) may be written as:

$$k(t) = e^{\kappa t} (a_1 \sin t + a_2 \cos t) - 2g\kappa_1, \quad (\text{A21})$$

where  $\kappa_1 = \kappa/(1 + \kappa^2)$ . By solving for  $s$  in the first parametric equation and plugging in, the result for  $k$  one has for  $s$ :

$$\begin{aligned} s(t) &= \dot{k} - \gamma k - 2g \\ &= e^{\kappa t} (-a_1 \cos t + a_2 \sin t) - 2g\kappa_2. \end{aligned} \quad (\text{A22})$$

where  $\kappa_2 = \kappa_1/\kappa$ . Thus, by doing the following change of variables;

$$k'(t) = k(t) - 2g\kappa_1, \quad (\text{A23})$$

$$s'(t) = s(t) - 2g\kappa_2 \quad (\text{A24})$$

then, we can describe the map given by the matrix  $\mathbf{R}$  given at (A12) to the primed variables exactly as we did for the diagonal element case, *i.e.* :  $\vec{r}'(t) = \mathbf{R}(t-t')\vec{r}'(t')$  where  $\vec{r}'(t) = \vec{r}(t) + 2g\vec{\kappa}$  and

$$\vec{\kappa} = \begin{pmatrix} \kappa_1 \\ \kappa_2 \end{pmatrix} = \frac{1}{1 + \kappa^2} \begin{pmatrix} \kappa \\ 1 \end{pmatrix}. \quad (\text{A25})$$

With these redefinitions, one can now write down the map which describes the motion of any point  $(k(t), s(t))$

along the characteristics as:

$$\vec{r}(t) = \mathbf{R}(t-t')\vec{r}(t') + 2g(\mathbf{R}(t-t') - \mathbb{1})\vec{\kappa}. \quad (\text{A26})$$

Integration of the third equation will yield

$$\begin{aligned} \int_{w_{01}(0)}^{w_{01}(t)} \frac{dw_{01}}{w_{01}} &= - \int_0^t dt' \left( i\Delta + \frac{\gamma_+}{2} |\vec{r}(t')|^2 \right), \\ &= -i\Delta t - \frac{\gamma_+}{2} \int_0^t dt' |\vec{r}(t')|^2. \end{aligned} \quad (\text{A27})$$

where  $|\vec{r}(t')|^2 = k^2(t') + s^2(t')$ . Now, we can use the map defined at (A26) to write  $k(\tau')$  and  $s(\tau')$  appearing in the integrand of the right hand side of (A27), as:

$$|\vec{r}(t')|^2 = |\mathbf{R}(t'-t)\vec{r}(t) + \vec{\eta}(t-t')|^2, \quad (\text{A28})$$

where

$$\vec{\eta}(t) = \frac{2g}{1 + \kappa^2} (\mathbf{R}(-t) - \mathbb{1}) \begin{pmatrix} \kappa \\ 1 \end{pmatrix} = - \begin{pmatrix} d_2(t) \\ d_1(t) \end{pmatrix}. \quad (\text{A29})$$

The last equality in this equation follows from direct evaluation of the integrals defined in Eq. (A17). Thus, by doing some algebra the integral in (A27) can be written as:

$$\begin{aligned} \int_0^t dt' |\vec{r}(t')|^2 &= \int_0^t dt' \left( |\mathbf{R}(-t')\vec{r}(t)|^2 \right. \\ &\quad \left. + 2\mathbf{R}^T(-t')\vec{\eta}(t') \cdot \vec{r}(t) + |\vec{\eta}(t')|^2 \right). \end{aligned} \quad (\text{A30})$$

Integration can be easily performed yielding for the non diagonal matrix element the following:

$$\begin{aligned} w_{01}(\vec{r}, t) &= w_{01}(\mathbf{R}(-t)\vec{r} + \vec{\eta}(t)) e^{-i\Delta t} \\ &\quad \exp \left[ -\frac{\gamma_+}{2} \alpha(t) |\vec{r}|^2 - \frac{\gamma_+}{2} \delta(t) \right] \\ &\quad \exp \left[ -\frac{\gamma_+}{2} \vec{\Gamma}(t) \cdot \vec{r} \right], \end{aligned} \quad (\text{A31})$$

where,

$$\delta(t) = \int_0^t dt' |\vec{\eta}(t')|^2, \quad (\text{A32})$$

$$\vec{\Gamma}(t) = 2 \int_0^t dt' \mathbf{R}^T(-t') \vec{\eta}(t'). \quad (\text{A33})$$

---

[1] S. A. Gardiner, J. I. Cirac, and P. Zoller, Phys. Rev. Lett. **79**, 4790 (1997).  
[2] A. Peres, Phys. Rev. A **30**, 1610 (1984).  
[3] H. M. Pastawski, P. R. Levstein, G. Usaj, J. Raya, and J. Hirschinger, Physica (Amsterdam) A **283**, 166 (2000).  
[4] T. Gorin, T. Prosen, T. H. Seligman, and M. Žnidarič, Phys. Rep. **435**, 33 (2006).

[5] P. Jacquod and C. Petitjean, Advances in Physics **58**, 67 (2009).  
[6] F. Binder, S. Vinjanampathy, K. Modi, and J. Goold, Phys. Rev. E **91**, 032119 (2015).  
[7] N. H. Y. Ng, L. Maninska, C. Cirstoiu, J. Eisert, and S. Wehner, New Journal of Physics **17**, 085004 (2015).  
[8] J. Millen and A. Xuereb, New Journal of Physics **18**, 011002 (2016).

- [9] J. Goold, M. Huber, A. Riera, L. del Rio, and P. Skrzypczyk, *J Phys A Math Theor* **49**, 143001 (2016).
- [10] S. Jevtic, D. Newman, T. Rudolph, and T. M. Stace, *Phys. Rev. A* **91**, 012331 (2015).
- [11] L. Mancino, M. Sbroscia, I. Gianani, E. Roccia, and M. Barbieri, *Phys. Rev. Lett.* **118**, 130502 (2017).
- [12] H. T. Quan, Y.-x. Liu, C. P. Sun, and F. Nori, *Phys. Rev. E* **76**, 031105 (2007).
- [13] R. Uzdin, A. Levy, and R. Kosloff, *Phys. Rev. X* **5**, 031044 (2015).
- [14] M. Horodecki and J. Oppenheim, *Nature Communications* **4**, 2059 (2013).
- [15] J. Anders and M. Esposito, *New Journal of Physics* **19**, 010201 (2017).
- [16] P. P. Hofer, J. B. Brask, M. Perarnau-Llobet, and N. Brunner, *Phys. Rev. Lett.* **119**, 090603 (2017).
- [17] T. Gorin, H. J. Moreno, and T. H. Seligman, *Philos. Trans. Royal Soc. A* **374**, 20150162 (2016).
- [18] M. A. Prado Reynoso, P. C. López Vázquez, and T. Gorin, *Phys. Rev. A* **95**, 022118 (2017).
- [19] G. M. Palma, K.-A. Suominen, and A. K. Ekertand, *Proc R Soc Lond A Math Phys Sci* **452**, 567 (1996).
- [20] J. H. Reina, L. Quiroga, and N. F. Johnson, *Phys. Rev. A* **65**, 032326 (2002).
- [21] C. van der Wal, F. Wilhelm, C. Harman, and J. Mooij, *Eur. Phys. J. B* **31**, 111 (2003).
- [22] F. Brito and T. Werlang, *New Journal of Physics* **17**, 072001 (2015).
- [23] A. C. S. Costa, M. W. Beims, and W. T. Strunz, *Phys. Rev. A* **93**, 052316 (2016).
- [24] A. Wallraff, D. I. Schuster, A. Blais, L. Frunzio, R.-S. Huang, J. Majer, S. Kumar, S. M. Girvin, and R. J. Schoelkopf, *Nature* **431**, 162 (2004).
- [25] I. Chiorescu, P. Bertet, K. Semba, Y. Nakamura, C. J. P. M. Harman, and J. E. Mooij, *Nature* **431**, 159 (2004).
- [26] R. Harris, M. W. Johnson, T. Lanting, A. J. Berkley, J. Johansson, P. Bunyk, E. Tolkacheva, E. Ladizinsky, N. Ladizinsky, T. Oh, F. Cioata, I. Perminov, P. Spear, C. Enderud, C. Rich, S. Uchaikin, M. C. Thom, E. M. Chapple, J. Wang, B. Wilson, M. H. S. Amin, N. Dickson, K. Karimi, B. Macready, C. J. S. Truncik, and G. Rose, *Phys. Rev. B* **82**, 024511 (2010).
- [27] A. Friedenauer, H. Schmitz, J. T. Glueckert, and T. Porras, D. and Schaetz, *Nature Physics* **4**, 757 (2008).
- [28] D. Porras, F. Marquardt, J. von Delft, and J. I. Cirac, *Phys. Rev. A* **78**, 010101 (2008).
- [29] K. Kim, S. Korenblit, R. Islam, E. E. Edwards, M.-S. Chang, C. Noh, H. Carmichael, G.-D. Lin, L.-M. Duan, C. C. J. Wang, J. K. Freericks, and C. Monroe, *New Journal of Physics* **13**, 105003 (2011).
- [30] P. Schindler, M. Müller, J. T. Nigg, D. and Barreiro, E. A. Martinez, M. Hennrich, T. Monz, S. Diehl, P. Zoller, and R. Blatt, *Nature Physics* **9**, 361 (2013).
- [31] J. Simon, W. S. Bakr, R. Ma, M. E. Tai, and M. Preiss, Philipp M. and Greiner, *Nature* **472**, 307 (2011).
- [32] A. Recati, P. O. Fedichev, W. Zwerger, J. von Delft, and P. Zoller, *Phys. Rev. Lett.* **94**, 040404 (2005).
- [33] P. P. Orth, I. Stanic, and K. Le Hur, *Phys. Rev. A* **77**, 051601 (2008).
- [34] P. Haikka, S. McEndoo, G. De Chiara, G. M. Palma, and S. Maniscalco, *Phys. Rev. A* **84**, 031602 (2011).
- [35] Y. Makhlin, G. Schön, and A. Shnirman, *Rev. Mod. Phys.* **73**, 357 (2001).
- [36] A. T. Sornborger, A. N. Cleland, and M. R. Geller, *Phys. Rev. A* **70**, 052315 (2004).
- [37] R. Betzholz, J. M. Torres, and M. Bienert, *Phys. Rev. A* **90**, 063818 (2014).
- [38] H. Scutaru, *J Phys A Math Theor* **31**, 3659 (1998).
- [39] A. Isar, *Physics of Particles and Nuclei Letters* **6**, 567 (2009).
- [40] A. Uhlmann, *Reports on Mathematical Physics* **9**, 273 (1976).
- [41] R. Jozsa, *Journal of Modern Optics* **41**, 2315 (1994).
- [42] A. A. Clerk and D. W. Utami, *Phys. Rev. A* **75**, 042302 (2007).
- [43] N. Zhao and Z.-q. Yin, *Phys. Rev. A* **90**, 042118 (2014).
- [44] V. Jagadish and A. Shaji, *Annals of Physics* **362**, 287 (2015).
- [45] A. O. Caldeira and A. J. Leggett, *Physica* **121A**, 587 (1983).
- [46] T. Gorin, T. Prosen, T. H. Seligman, and W. T. Strunz, *Phys. Rev. A* **70**, 042105:1 (2004).
- [47] E. C. G. Sudarshan, P. M. Mathews, and J. Rau, *Phys. Rev.* **121**, 920 (1961).
- [48] V. Gorini, A. Kossakowski, and E. C. G. Sudarshan, *Journal of Mathematical Physics* **17**, 821 (1976).
- [49] G. Lindblad, *Commun. Math. Phys.* **48**, 119 (1976).
- [50] H. J. Moreno, T. Gorin, and T. H. Seligman, *Phys. Rev. A* **92**, 030104 (2015).
- [51] A. M. de Almeida, *Physics Reports* **295**, 265 (1998).
- [52] A. M. O. de Almeida, *J Phys A Math Gen* **36**, 67 (2003).
- [53] O. Brodier and A. M. O. d. Almeida, *Phys. Rev. E* **69**, 016204 (2004).
- [54] H. P. Breuer and F. Petruccione, *The Theory of Open Quantum Systems* (Oxford University Press, USA, 2002).
- [55] H. Weyl, *Zeitschrift für Physik* **46**, 1 (1927).
- [56] A. B. Klimov and S. M. Chumakov, *A Group-Theoretical Approach to Quantum Optics* (Wiley-VCH Verlag GmbH and Co. KGaA, 2009).
- [57] I. Rigas, L. Sanchez-Soto, A. Klimov, J. ehek, and Z. Hradil, *Annals of Physics* **326**, 426 (2011).
- [58] W. B. Case, *American Journal of Physics* **76**, 937 (2008).
- [59] R. R. Puri and G. S. Agarwal, *Phys. Rev. A* **35**, 3433 (1987).
- [60] F. Haug, M. Bienert, W. P. Schleich, T. H. Seligman, and M. G. Raizen, *Phys. Rev. A* **71**, 043803:1 (2005).